2024 IEEE PES Generation, Transmission and Distribution Latin America Conference and Industrial Exposition (GTDLA) | 979-8-3315-3054-9/24/$31.00 ©2024 IEEE | DOI: 10.1109/GTDLA61236.2024.10913872

Boosting Resilience in Power Distribution Systems using Compensated Distance Relays

S. Pérez-Londoño, *Member, IEEE*
Electrical Engineering Program
Universidad Tecnológica de Pereira
Pereira, Colombia
saperez@utp.edu.co

S. Velasco-Gómez
Electrical Engineering Program
Universidad Tecnológica de Pereira
Pereira, Colombia
sary.m.gomez@utp.edu.co

***Abstract*—Power system resilience is the ability of an electrical power system to withstand and quickly recover from disruptive and high-impact events such as natural disasters, equipment failures, cyberattacks, or other emergencies while maintaining its critical functions. Many proposals consider resilience metrics to evaluate the performance of a power system under these extreme events. Still, most proposals consider the resilience of the high-voltage bulk power grid. Still, there are few medium-voltage and power distribution systems. Therefore, it does not assess the resilience of specific elements considered essential in distribution networks as the protection system.**

This paper proposes and evaluates a time-based quantitative metric to determine the power system resilience when compared to a conventional and a compensated distance-based relay. Using such a protection function is justified, as the new challenges in active distribution networks nowadays force different protection to overcome the issues of typical overcurrent relays.

Simulation on a modified IEEE34-bus system is employed to validate the effectiveness of a compensated distance-based relay. The results show how compensated relays' response time can be improved over conventional protections, which enhances system resilience.

***Keywords*—Distance-based protection, resilience index, conventional protection, relay operating time.**

I. Introduction

A. Motivation

The word "resilience" has been used for several decades [1], [2]; however, its usage has gained more prominence in power systems during recent years, especially with the increasing occurrence of climate-related extreme events and society's growing dependence on electricity [3], [4].

Electrical system operation can be affected by extreme events, such as natural disasters (hurricanes and cyclones, tornadoes, floods, earthquakes) or cyberattacks, that cause widespread power outages and significant economic losses. In response to these events and changes in energy infrastructure, policies, regulations, and technologies have been developed to enhance the resilience of electrical systems.

Some strategies for enhancing the power system's resilience include smartening the network, which considers advanced technologies, metering, and communication services. This is possible through the integration of microgrids, distributed generators (DGs), energy storage systems (ESS), and electric vehicles (EVs) for service restoration. DGs and microgrids are used as sources to provide services to critical loads on neighboring feeders. Microgrid is a concept that contributes to improving resilience; however, including these technologies implies new challenges to the electric network, such as cybersecurity, control and management, grid stability, and grid protection, among others.

Several papers have demonstrated that typical overcurrent relay-based strategies are insufficient in microgrids, given specific characteristics such as bidirectional load flows, unbalanced loads, and X/R levels [5], [6]. For this reason, all proposals concerning detecting outage locations, improving conventional schemes, and reducing the time customers are affected by extreme events are highly significant. However, developing new protection strategies is insufficient if resilience enhancement is not quantitatively evaluated. Therefore, this paper proposes a time-based resilience metric of easy application that can be specially used to validate new distance-based protection proposals.

B. State of the art

Resilience is a multidimensional concept that considers many factors; therefore, there is a lack of consensus surrounding its definition in electric systems. Despite this, several methods exist for analyzing and quantifying resilience. One corresponds to resilience metrics, which measure a system's ability to withstand and recover from disruptions, shocks, or stresses while maintaining functionality and performance. Metrics can be quantitative or qualitative, and although many resilience metrics are used in literature, no standardized metrics are available to evaluate a grid's resilience [7]. Some grid's resilience strategies use metrics adopted from reliability indicators such as Loss of Load Frequency (LOLF), Loss of Load Expectation (LOLE), Loss of Load Probability (LOLP), System Average Interruption Frequency Index (SAIFI), and the System-Average Interruption Duration Index (SAIDI) [8]. However, many authors consider using them inappropriate. They measure a system's capacity in the face of different events with different probabilities [9].

In quantitative evaluation, there are time-dependent metrics for the resilience of power networks based on slopes and area of resilience triangle [10] and resilience trapezoid indicated in fig 1 [11]. For example, under an extreme event, Panteli et al., [12] proposes the FLEP metric, where the resilience is evaluated during the degradation phase through the falling slope between degradation time t_0 to and post-event time t_1. Similarly, [13] proposes a Degradation Index (DI), but detailed information on resilience curve behaviour is required. In [14], the area under the real performance is used, which can be normalized with the area under the ideal performance curve.

Some resilience metrics employing comparison resources availability before and after the event (power plant generation difference before and after event [15], number of online or offline transmission/distribution lines [12], number of connected or disconnected customers [16], [17] or affected substations [9]). Other metrics include specific variables such as weather events (intensity) and the physical resilience of infrastructure, which cannot help evaluate enhancement schemes based on electrical protections.

Recent papers, as presented in [18], propose stochastic models of the outages and restores, as Poisson processes, to define performance curves whose parameters can be estimated from data recorded by utilities. Then, the curves' area, nadir, and duration are used as resilience metrics.

Due to the number of proposals on resilience, a resilience metric must be adapted to a specific condition or proposal to be usable. According to the literature revision, no specific resilience metric proposals related to electrical protection systems allow validation of the improvements that could have been made.

C. Contributions

This paper proposes a metric indicator for evaluating resilience performance when compensated distance-based protection is used in a distribution network. This protection function is proposed to overcome the issues widely reported of typical overcurrent protection.

II. Role of Protecting Devices in the System Resilience

According to the literature, there are two grid resilience frameworks: grid assessment and grid enhancement [19]. In the former, the weather and the grid information are used to evaluate the grid's operational condition. Several studies consider that the resilience performance level during disruptive events can be estimated as a function of the system's robustness (R) and rapidness (Δt) through four stages of the resilience trapezoid, as shown in Fig. 1.

The robustness of an electrical system refers to its ability to withstand and recover from various disturbances, faults, and adverse conditions while maintaining its functionality, stability, and performance. A robust electrical system can resist disruptions, adapt to changing conditions, and continue to provide reliable power supply to consumers. This includes withstanding events like equipment failures, overloads, voltage fluctuations, short circuits, extreme weather, and external threats like cyberattacks or physical sabotage. Additionally, a robust electrical system should quickly detect and isolate faults, restore power after outages, and maintain grid stability

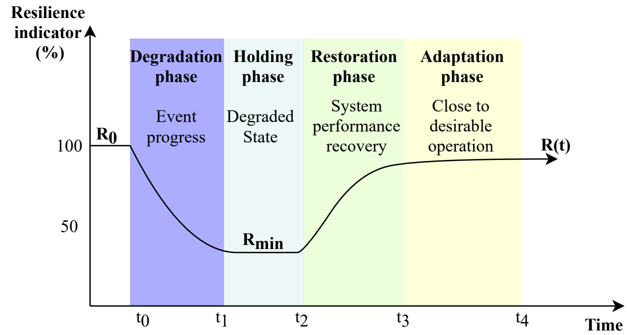

Fig. 1: Typical resilience curve

to ensure the continuity of operations and minimize disruptions to users. The lower the robustness, the more functionality loss is achieved and, therefore, the less resilient the system is. According to Fig 1, the resilience during the Degradation phase, the network experiences the event's impact, challenging the grid's robustness. This necessitates swift coordination among various elements to withstand the load demand during the Holding phase. Lastly, restorative action can occur to reach the desirable operation in the Adaption phase.

Protecting devices, such as relays and circuit breakers, play a critical role in enhancing the resilience of electrical systems by promptly detecting and isolating faults and abnormal conditions, minimizing downtime, maintaining system stability, protecting equipment, and facilitating the restoration process. These devices serve as the first line of defence and are some elements mainly responsible for minimizing network robustness loss during the resilience curve's Degradation phase.

A. Resilience and protecting relaying relationship

During a high-impact and low-frequency (HILF) event, severe electrical infrastructure damage may occur, such as multiple faults or outages of power equipment such as lines, generators, or loads.

In such cases where the protection scheme is not adapted to the specific conditions presented in the power grid, such as DG or ESS inclusion, bidirectional active power flows, line unbalance, and different fault resistances, among others, must be solved. The typical overcurrent protection-based strategies present inadequate operation, originating false tripping, delays and directional issues, conducing to cascading outages, and compromising the stability of the entire network, leading to a collapse during a HILF event [20]. Thus, designing a resilient protection system against all these issues is critical to improving the system's resilience.

B. Conventional and compensated protection of electric power systems

Conventional protection of power lines typically considers non-pilot overcurrent, distance, and differential relays [21]. This paper deals with conventional and compensated distance-based relays, mainly considering the common unbalance of electric distribution systems [22], as these can solve overcurrent protection issues. Additionally, distance relays do not represent high additional costs as the directional overcurrent relays require potential protection transformers, which can be used in the new proposed compensated distance relays.

Conventional distance protection defines its operation depending on the estimated positive sequence impedance (Z_e^1) from the relay location to the fault point at a distance d. This protection function generates a trip order when Z_e^1 is lower than the zone setting impedance (Z_{set}^1) [23]. Fig 2 presents the standard zones defined for the distance relay calibration (Distance relay located at node M). The equation in (1) is used to determine Z_e^1 for single line to ground faults, while equation (2) is used for phase faults [24].

$$Z_{e_{\zeta g}}^1 = \frac{U_{r_\zeta}}{I_{r_\zeta} + k_0 I_r^0} \tag{1}$$

$$Z_{e_{\zeta\psi}}^1 = \frac{U_{r_\zeta} - U_{r_\psi}}{I_{r_\zeta} - I_{r_\psi}} \tag{2}$$

Where $\zeta \wedge \psi \in (a, b, c)$, and U_{r_ζ} and I_{r_ζ} are phase voltage and line current at phase ζ measured by the relay. k_0 is a defined in (3), as in [21], and I_r^0 is the zero-sequence current. z^0 and z^1 are the per unit length zero and positive sequence line impedances, respectively.

$$k_0 = \frac{z^0 - z^1}{z^1} \tag{3}$$

Finally, the estimated fault distance d_e is obtained as Z_e^1/z^1, where z^1 is the per unit positive line sequence impedance.

Improved distance-based relays for unbalanced power systems are based on the conventional relay, but the estimation of Z_e^1 considers an unbalanced system. In the case of the system depicted in figure Fig. 3, relay voltage during a fault on an

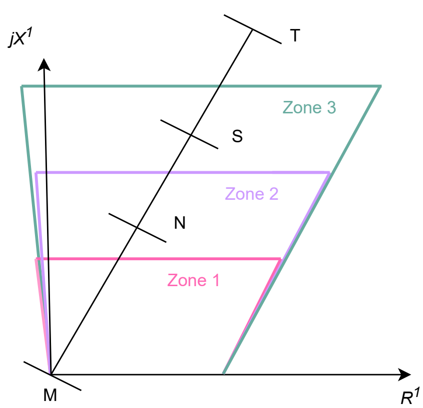

Fig. 2: Commonly zones defined for the node M located distance relay calibration

unbalanced line depends on the line drop voltage ($\mathbf{\Delta U}_{l_{abc}}$) and the fault voltage ($\mathbf{U}_{f_{abc}}$), as presented in (4).

$$\mathbf{U}_{r_{abc}} = \mathbf{\Delta U}_{l_{abc}} + \mathbf{U}_{f_{abc}} \tag{4}$$

The expression in (5) can be obtained for a ag single phase

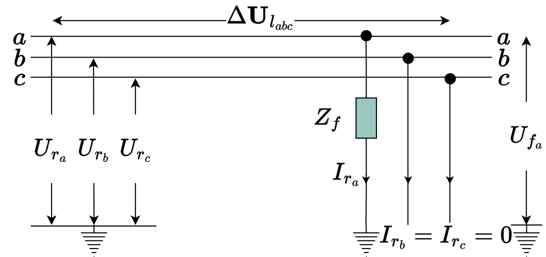

(a) SLG fault.

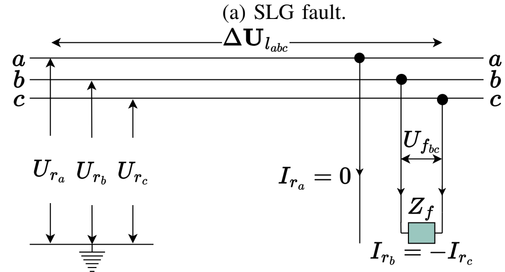

(b) LL fault.

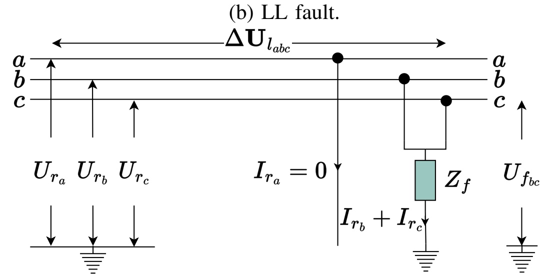

(c) LL-G fault.

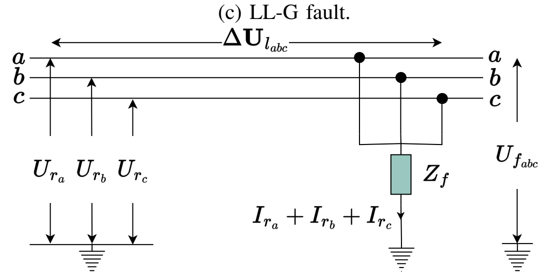

(d) LLL-G fault.

Fig. 3: Faulted electric power lines.

to ground fault at a distance d, as presented in Fig 3a, by analyzing (4) considering an unbalanced line.

$$U_{r_a} = \Delta U_{l_a}^0 + \Delta U_{l_a}^1 + \Delta U_{l_a}^2 + U_{f_a} = 3I_{r_a}^0 \left(Z_{aa} + Z_f\right) \tag{5}$$

The per-unit impedance (z_{aa}) is defined as $z_{aa} = \frac{Z_{aa}}{d}$; then, considering $3I_{r_a}^0 = I_{r_a}$ and (5), the estimated distance (d_e) for bolted single-phase to ground faults in phase a is defined in (6).

$$d_e = \left| \frac{U_{r_a}}{I_{r_a}\, z_{aa}} \right| \tag{6}$$

Performing a similar analysis as the one presented in equation (5), in the case of a bc double-phase fault as the one presented in Fig.3b, the estimated fault distance d_e is obtained as (7). The same analysis is applied for ab and ca faults.

$$d_e = \left| \frac{U_{r_b} - U_{r_c}}{(I_{r_b} - I_{r_c})(z_{aa} - z_{bc})} \right| \tag{7}$$

In the case of a bcg double phase to ground fault as presented in Fig. 3c, the compensated fault distance d_e is the same as the obtained in presented in (7).

In the case of $abcg$ three-phase to ground faults and from the analysis of Fig.3d results in equation (8) the estimated fault distance.

$$d_e = \left| \frac{U_{r_a}}{z_{aa}I_{r_a} + z_{ab}I_{r_b} + z_{ca}I_{r_c}} \right| \tag{8}$$

Finally, the total impedance estimated by the relay is presented as $Z_e^1 = d_e z_{aa}$.

III. Methodology to evaluate the system resilience

The proposed approach evaluates the protection system operating time by defining a resilience index based on the time required to clear the faulted system.

In this case, the resilience index is defined by the relay operating times, as is presented in (9); where t_{op} is the current accumulative protection system operating time, while t_{op}^e is the expected accumulative protection system operating time, as is defined in (10). ϵ is a positive value used to avoid undefined mathematical expressions, especially in the case of zone 1 relay operation, where $t_{op}^e = 0$ [ms]; $\epsilon \in \Re^+$.

$$Ri_t = \frac{t_{op}^e + \epsilon}{t_{op} + \epsilon} \tag{9}$$

$$t_{op} = \sum_{r=0}^{N} t_{op_r} \qquad t_{op}^e = \sum_{r=0}^{N} t_{op_r}^e \tag{10}$$

In (10), N is the number of total relays which has to operate in the case of a HILF event; t_{op_r} and $t_{op_r}^e$ are the actual operating time for and the expected operating time, respectively, for all relays ($r \in N$).

The complete resilience evaluation methodology is based on defining probable HILF scenarios to determine the expected Ri_t index of the analyzed protection system. In the case of outstanding performance, the index is close to unity, while in the case of poor performance, it reduces its value.

Finally, the proposal considers the following stages: *i)* Calibration of all N relays in the analyzed system, *ii)* Determination of the expected operating times ($t_{op_r}^e$), *iii)* Definition of the most probable HILF scenarios, *iv)* Determination of the relay operating times, and *v)* Resilience index calculation.

IV. Analysis of the results

A. Test system

The system used for tests is a modification of the IEEE 34-nodes distribution network depicted in Fig. 4. It includes several compensated distance relays, as presented in section II.B.

TABLE I: Distance relay zone calibration

Relay	Relay zones impedance $\|Z_{set}^1\|[\Omega]$ 1	2	3
R_{808}	19.660	24.740	41.641
R_{816}	3.217	21.598	27.141
R_{828}	20.027	23.713	24.051

B. Testing scenarios

The analyzed test includes two HILF scenarios: a) four simultaneous faults located downstream of the relay at node 808 (R_{808}), and b) three simultaneous faults located downstream of the relay at node 828 (R_{808}). In both cases, three fault resistances (0, 20, and 50 [Ω]) and two fault types (single phase to ground and phase phase faults) are considered. The closest fault (f_1) to relay R_{808} is located at approximately 87% of the line 808-816 length (16 miles) for scenario a, while the closest fault (f_2) to relay R_{828} is located at approximately 70% of the line 828-842 length (9.1 miles).

Finally, the quadrilateral zone distance relay is calibrated using the 90% criterion. As examples, the relay 808 has the following settings: zone 1 reaches $0.9Z_{808-816}$, zone 2 reaches $Z_{808-816} + 0.81Z_{816-828}$, and zone 3 reaches $Z_{808-816} + Z_{816-828} + 0.72Z_{828-834}$; relay 828 is calibrated using $0.9Z_{828-834}$, zone 2 reaches $Z_{828-834} + 0.81Z_{834-848}$, and zone 3 reaches $Z_{828-848}$. Table I present the settings of relays R_{808}, R_{816} and R_{828}.

Zones 1, 2, and 3's expected operating times for all distance relays are 0, 200, and 400 [ms], respectively.

C. Results and analysis

1) Scenario a: four simultaneous faults downstream relay R_{808}: In this testing scenario, the expected relay operation indicates that only relay R_{808} must operate in zone 1. The obtained results at this considered testing scenario are presented in Table II, for the compensated impedance estimation (Z_{comp}) and the conventional distance estimation (Z_{conv}).

According to the obtained results and considering a quadrilateral relay calibrated at 90% of the line impedance ($Z_{\text{zone}_1} = 19.669\underline{/32.948°}$), in the case of 0 [$\Omega$] faults, both relays (compensated and conventional) operate in zone 1. However, in the case of 20 and 50 [Ω] faults, only the compensated relay operates in zone 1, and the conventional relay operates in zone 2 or 3. The proposed index is then estimated only considering relay R_{808}, and the results are presented in Table III. In all cases, ϵ is defined as 0.1 to avoid mathematical indetermination in (9).

As shown in Table III, the resilience index is lower for such cases where the presence of a fault resistance is notorious. In the cases of single and double-faulted phases and for 20 and 50 [Ω] fault resistances, the trip zones of the conventional distance relay are Zone 2 and Zone 3, respectively. Consequently, Ri_t is lower in the cases of fault resistance, degrading the quality of the system protection and then exposing the protected system to longer fault times. Finally, the faulted zone is adequately

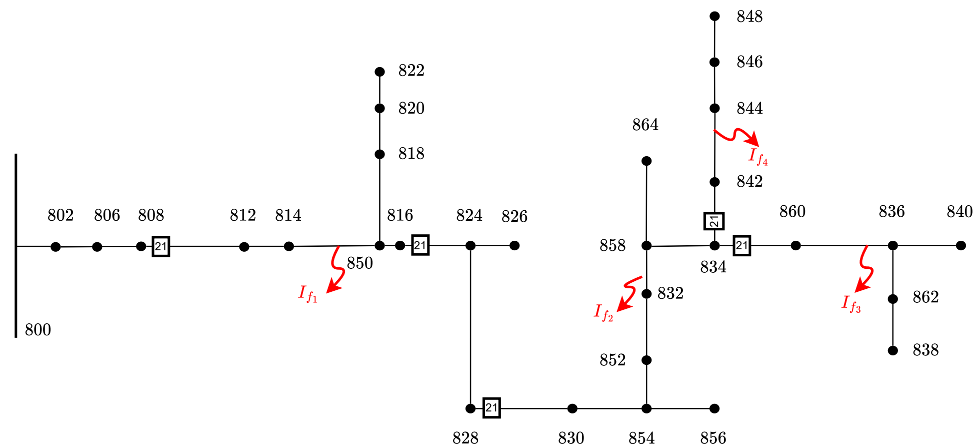

Fig. 4: A four faults HILF event at the IEEE 34 nodes based test system

TABLE II: Estimated impedance by R_{808} for a HILF event (Scenario *a*)

$Z_{estimated}$	Impedance estimated by relay R_{808}		R_f
	Single phase fault	Phase phase fault	
Z_{conv}	$19.368\angle 32.432°$	$19.334\angle 32.952°$	0 [Ω]
Z_{copm}	$19.166\angle 32.356°$	$19.086\angle 31.408°$	
Z_{conv}	$37.501\angle 16.153°$	$38.032\angle 16.975°$	20 [Ω]
Z_{copm}	$19.273\angle 31.826°$	$19.318\angle 32.007°$	
Z_{conv}	$66.861\angle 8.937°$	$68.296\angle 8.103°$	50 [Ω]
Z_{copm}	$19.501\angle 30.176°$	$19.470\angle 29.997°$	

TABLE III: Estimated resilience index (Ri_t)

Estimation	Ri_t based on relay R_{808}		R_f
	Single phase fault	Phase phase fault	
Conventional	1.000	1.000	0 [Ω]
Compensated	1.000	1.000	
Conventional	0.334	0.334	20 [Ω]
Compensated	1.000	1.000	
Conventional	0.200	0.200	50 [Ω]
Compensated	1.000	1.000	

identified in the case of the compensated relay and for all the tested cases; consequently, Ri_t estimated as presented in (9) is always equal to the unity.

2) Scenario b: three simultaneous faults downstream relay 828: In this scenario, the expected operation considers a determination of a zone 1 fault in R_{828}, zone 2 fault in R_{816}, and zone 3 fault in R_{808}, according to the obtained results and considering quadrilateral relays calibrated as presented in Table I.

The identified zones for relay R_{828} are presented in Table IV for Z_{comp} and Z_{conv}. As in the previous scenario, in the case of 0 [Ω] faults, both relays (compensated and conventional) operate in zone 1. However, in the case of 20 and 50 [Ω] faults, only the compensated relay operates in zone 1, and the conventional relay operates in zone 2 or 3.

In this scenario, as relays R_{828}, R_{816} and R_{808} must identify the fault in zones 1, 2, and 3, respectively, the proposed index is estimated considering those relays as presented in Table V.

TABLE IV: Estimated impedance by R_{828} for a HILF event (Scenario *b*)

$Z_{estimated}$	Impedance estimated by relay R_{828}—		R_f
	Single phase fault	Phase phase fault	
Z_{conv}	$15.568\angle 32.981°$	$15.573\angle 32.976°$	0 [Ω]
Z_{copm}	$15.573\angle 32.376°$	$15.569\angle 32.908°$	
Z_{conv}	$34.501\angle 15.201°$	$35.032\angle 14.215°$	20 [Ω]
Z_{copm}	$15.573\angle 30.103°$	$15.573\angle 32.126°$	
Z_{conv}	$63.891\angle 8.001°$	$64.951\angle 7.992°$	50 [Ω]
Z_{copm}	$15.573\angle 31.243°$	$15.573\angle 28.948°$	

TABLE V: Estimated resilience index (Ri_t)

Estimation	Ri_t based on relays R_{808}, R_{816} and R_{828}		R_f
	Single phase fault	Phase phase fault	
Conventional	1.000	1.000	0 [Ω]
Compensated	1.000	1.000	
Conventional	0.000	0.000	20 [Ω]
Compensated	1.000	1.000	
Conventional	0.200	0.000	50 [Ω]
Compensated	1.000	1.000	

As shown in Table V, the resilience index is zero for cases where a fault resistance is notorious. In the cases of single and double-faulted phases and for 20 and 50 [Ω] fault resistances, conventional relay R_{808} does not identify the presence of a fault, then the tripping time is infinite, leading to a zero Ri_t. Finally, and as presented in scenario *a*, the faulted zone is adequately identified in the case of the compensated relay and for all the tested cases; consequently, Ri_t estimated as presented in (9) is always equal to the unity.

V. Conclusions

An adequate protection system can improve the resilience of an electric power system. In this case, the distance relay is the protecting device, considering two relay approaches: conventional and compensated. A resilience index is also defined based on the expected and current relay operating times. As demonstrated by tests, considering single and phase-to-phase faults and several fault resistances, the compensated relay can adequately determine the faulted zone even in the case of simultaneous faults (HILF event), maintaining a high resilience index.

Currently, there are no specific proposals in the literature to determine a device's impact on a system's resilience (such as the distance relay), so there is no way to compare it. This proposal is presented as an opportunity to continue developing indicators.

Finally, the proposed index can consider evaluating all the protection systems, concluding that a value lower than the unity means longer relay operating times and the consequent equipment degradation due to longer fault times.

Acknowledgment

This paper results from the research program Integra2023, funded by Minciencias-Colombia. The research group ICE3 at the Universidad Tecnológica de Pereira obtained this product.

References

[1] A. K. Srivastava, C.-C. Liu, and S. Chanda, *Resiliency of Power Distribution Systems*. John Wiley & Sons, 2023.

[2] A. Younesi, H. Shayeghi, Z. Wang, P. Siano, A. Mehrizi-Sani, and A. Safari, "Trends in modern power systems resilience: State-of-the-art review," *Renewable and Sustainable Energy Reviews*, vol. 162, p. 112397, 2022.

[3] D. M. Ward, "The effect of weather on grid systems and the reliability of electricity supply," *Climatic Change*, vol. 121, no. 1, pp. 103–113, 2013.

[4] N. Abi-Samra, J. McConnach, S. Mukhopadhyay, and B. Wojszczyk, "When the bough breaks: Managing extreme weather events affecting electrical power grids," *IEEE Power and Energy Magazine*, vol. 12, no. 5, pp. 61–65, 2014.

[5] A. Barranco-Carlos, C. Orozco-Henao, J. Marín-Quintero, J. Mora-Flórez, and A. Herrera-Orozco, "Adaptive protection for active distribution networks: An approach based on fuses and relays with multiple setting groups," *IEEE Access*, vol. 11, pp. 31 075–31 091, 2023.

[6] G. Muñoz-Arango, J. Mora-Flórez, and S. Pérez-Londoño, "Optimal data-driven adaptive overcurrent relay coordination for active distribution networks," *Electric Power Systems Research*, vol. 228, p. 110078, 2024.

[7] S. Ahmadi, Y. Saboohi, and A. Vakili, "Frameworks, quantitative indicators, characters, and modeling approaches to analysis of energy system resilience: A review," *Renewable and Sustainable Energy Reviews*, vol. 144, p. 110988, 2021.

[8] M. Panteli and P. Mancarella, "Modeling and evaluating the resilience of critical electrical power infrastructure to extreme weather events," *IEEE Systems Journal*, vol. 11, no. 3, pp. 1733–1742, 2015.

[9] H. Raoufi, V. Vahidinasab, and K. Mehran, "Power systems resilience metrics: A comprehensive review of challenges and outlook," *Sustainability*, vol. 12, no. 22, p. 9698, 2020.

[10] W. Kröger, "Achieving resilience of large-scale engineered infrastructure systems," *Resilient structures and infrastructure*, pp. 289–313, 2019.

[11] D. K. Mishra, M. J. Ghadi, L. Li, J. Zhang, and M. Hossain, "Active distribution system resilience quantification and enhancement through multi-microgrid and mobile energy storage," *Applied Energy*, vol. 311, p. 118665, 2022.

[12] M. Panteli, P. Mancarella, D. N. Trakas, E. Kyriakides, and N. D. Hatziargyriou, "Metrics and quantification of operational and infrastructure resilience in power systems," *IEEE Transactions on Power Systems*, vol. 32, no. 6, pp. 4732–4742, 2017.

[13] M. Amirioun, F. Aminifar, H. Lesani, and M. Shahidehpour, "Metrics and quantitative framework for assessing microgrid resilience against windstorms," *International Journal of Electrical Power & Energy Systems*, vol. 104, pp. 716–723, 2019.

[14] H. Gao, Y. Chen, Y. Xu, and C.-C. Liu, "Resilience-oriented critical load restoration using microgrids in distribution systems," *IEEE Transactions on Smart Grid*, vol. 7, no. 6, pp. 2837–2848, 2016.

[15] M. Panteli, D. N. Trakas, P. Mancarella, and N. D. Hatziargyriou, "Power systems resilience assessment: Hardening and smart operational enhancement strategies," *Proceedings of the IEEE*, vol. 105, no. 7, pp. 1202–1213, 2017.

[16] Z. Bie, Y. Lin, G. Li, and F. Li, "Battling the extreme: A study on the power system resilience," *Proceedings of the IEEE*, vol. 105, no. 7, pp. 1253–1266, 2017.

[17] S. Lei, J. Wang, C. Chen, and Y. Hou, "Mobile emergency generator pre-positioning and real-time allocation for resilient response to natural disasters," *IEEE Transactions on Smart Grid*, vol. 9, no. 3, pp. 2030–2041, 2016.

[18] I. Dobson, "Models, metrics, and their formulas for typical electric power system resilience events," *IEEE Transactions on Power Systems*, 2023.

[19] S. Afzal, H. Mokhlis, H. A. Illias, N. N. Mansor, and H. Shareef, "State-of-the-art review on power system resilience and assessment techniques," *IET Generation, Transmission & Distribution*, vol. 14, no. 25, pp. 6107–6121, 2020.

[20] S. Mishra, K. Anderson, B. Miller, K. Boyer, and A. Warren, "Microgrid resilience: A holistic approach for assessing threats, identifying vulnerabilities, and designing corresponding mitigation strategies," *Applied Energy*, vol. 264, p. 114726, 2020.

[21] P. M. Anderson, C. F. Henville, R. Rifaat, B. Johnson, and S. Meliopoulos, *Power system protection*. John Wiley & Sons, 2022.

[22] S. Velasco-Gómez, S. Perez-Londono, and J. Mora-Floréz, "Unbalance compensated distance relay for active distribution networks," *Energy Reports*, vol. 9, pp. 438–446, 2023.

[23] A. Hooshyar and R. Iravani, "Microgrid protection," *Proceedings of the IEEE*, vol. 105, no. 7, pp. 1332–1353, 2017.

[24] C. García-Ceballos, S. Pérez-Londoño, and J. Mora-Flórez, "Compensated fault impedance estimation for distance-based protection in active distribution networks," *International Journal of Electrical Power & Energy Systems*, vol. 151, p. 109114, 2023.